MOF Nanosheet Reconstructed Two-Dimensional Bionic Nanochannel for Protonic Field-Effect Transistors

Guo-Dong Wu[+], Hai-Lun Zhou[+], Zhi-Hua Fu, Wen-Hua Li, Jing-Wei Xiu, Ming-Shui Yao, Qiao-hong Li,* and Gang Xu*

Abstract: *The construction of hydrophobic nanochannel with hydrophilic sites for bionic devices to proximally mimick real bio-system is still challenging. Taking the advantages of MOF chemistry, a highly oriented CuTCPP thin film has been successfully reconstructed with ultra-thin nanosheets to produce abundant two-dimensional interstitial hydrophobic nanochannels with hydrophilic sites. Different from the classical active-layer material with proton transport in bulk, CuTCPP thin film represents a new type of active-layer with proton transport in nanochannel for bionic proton field-effect transistor (H+-FETs). The resultant device can reversibly modulate the proton transport by varying the voltage on its gate electrode. Meanwhile, it shows the highest proton mobility of $\approx 9.5 \times 10^{-3}$ $cm^2 V^{-1} s^{-1}$ and highest on-off ratio of 4.1 among all of the reported H+-FETs. Our result demonstrates a powerful material design strategy for proximally mimicking the structure and properties of bio-systems and constructing bionic electrical devices.*

Controlled proton transport in nanochannel is critical for the bio-systems, such as cytochrome c oxidase proton pump, bacteriorhodopsin, and cytochrome P450 monooxygenases.[1] Biomimetic devices that can reversibly modulate proton transport are of great importance to not only interface with bio-systems, but also understand the working mechanisms of these bio-systems.[2] For this purpose, protonic filed-effect transistors (H+-FETs) have become a research focus in these years.[3,4] The active layer is the critical part of H+-FETs in mimicking the proton transport of bio-system. Many hydrophilic materials, including maleic chitosan, cephalopod structural protein, porous organic polymer, etc., have been successfully studied as active layers.[3a–c] However, in bio-systems, proton transport nanochannels normally require hydrophobic body for stabilizing them structure in cellular fluid but hydrophilic sites for efficient protons transfer (Scheme 1).[5] Thus, for proximally mimicking the bio-channel in both structure and function, a hydrophobic body-hydrophilic sites structure is required, while has not been realized by the reported hydrophilic materials. Moreover, most of the reported H+-FETs have a bulk active layer which is also different from the nano-channel structure in bio-system.[3,4] New materials that can be used to construct nanochannels with hydrophobic body-hydrophilic sites structure is extremely desired.

Metal-organic frameworks (MOFs) are a type of crystalline materials constructed with long-range ordered inorganic nodes and organic bridging ligands.[6] The existence of the enormous library of inorganic and organic building units as well as diverse combination modes of them endows MOFs with great flexibility in structure design for desired properties.[7] Therefore, MOFs have attracted intensive research interest for proton conduction.[8] MOFs with conductivity higher than 10^{-1} $S cm^{-1}$ or working temperature higher than 150°C have been successfully designed and prepared.[9] More importantly, MOFs are a judicious selection to mimic the biochannels with hydrophobic boy-hydrophilic sites structure. The elaborately selected organic ligand can provide large hydrophobic regions in the MOFs, while the inorganic nodes can be designed with high hydrophilicity. Despite these favored features, MOF active-layer based H+-FET has not been reported yet.

[*] Dr. G. D. Wu,[+] H. L. Zhou,[+] Dr. Z. H. Fu, Dr. W. H. Li, J. W. Xiu, Dr. M. S. Yao, Prof. Q. H. Li, Prof. G. Xu
State Key Laboratory of Structural Chemistry, Fujian Institute of Research on the Structure of Matter, Chinese Academy of Sciences
155 Yangqiao Road West, Fuzhou, Fujian, 350002 (China)
E-mail: lqh2382@fjirsm.ac.cn
gxu@fjirsm.ac.cn

Prof. G. Xu
University of Chinese Academy of Sciences
Beijing 100049 (China)
and
Fujian Science & Technology Innovation Laboratory for Optoelectronic Information of China
Fuzhou, Fujian 350108 (China)

[+] These authors contributed equally to this work.

Supporting information and the ORCID identification number(s) for the author(s) of this article can be found under:
https://doi.org/10.1002/anie.202100356.

a Proton transport in hydrophobic bio-channel
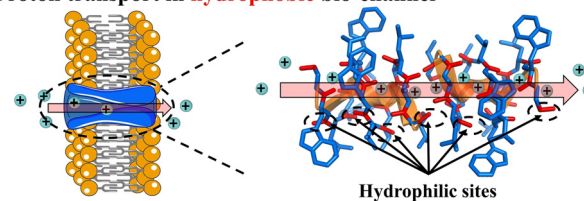
Hydrophilic sites

b Proton transport in bionic FETs

PdHx | PdHx | PdHx | PdHx

SiO₂/Si | SiO₂/Si
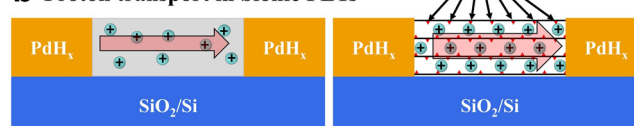
Reported: hydrophilic bulk materials | New: hydrophobic bionic-nanochannels

Scheme 1. Proton transport in a) bio-systems and b) biomimetic H+-FETs.

In this work, MOF materials were employed as the active-layer to fabricate H⁺-FET device for the first time. A well-known MOF, Cu-TCPP, was rationally selected for the following reasons: 1) it can be easily prepared into ultrathin nanosheet for reassembling thin film with abundant interstitial nanochannels for mimicking the proton transport in the nanochannels of bio-systems;[10] 2) it possesses good proton conductivity while ultra-low electronic conductivity, which is a favorable active-layer material to H⁺-FET;[11] 3) its aromatic porphyrin ligand and inorganic Cu paddle-wheel node can provide large hydrophobic region and hydrophilic open metal site, respectively, for best approaching the hydrophobic-hydrophilic structure of bio-channels. The obtained thin film successfully mimics the structure and function of bio-channels. Electrical measurements reveal this MOF thin film H⁺-FET not only shows physically modulated proton transport, but also possesses a mobility of $\approx 9.5 \times 10^{-3}$ $cm^2 V^{-1} s^{-1}$ and on-off ratio of ≈ 4.1, both of which are the highest values in the reported H⁺-FET.

Cu-TCPP shows a reticular layered structure in *ab* plane, where Cu centered porphyrin rings are connected with each other by $Cu_2(COO)_4$ paddle-wheel structures (Figure 1a).[12] This structure orderly arranges the large-area hydrophobic porphyrin molecules and hydrophilic coordination unsaturated Cu atoms in long range. Neighboring layers parallelly stack along *c* axis through weak interactions. The layered structure benefits the preparation of ultrathin nanosheet. Crystalline ultrathin Cu-TCPP nanosheets were prepared in high-yield by a solution reaction between $Cu(NO_3)_2 \cdot 3H_2O$ and H_2TCPP (5, 10, 15, 20-tetrakis (4-carboxyphenyl) porphyrin).[13a] As shown in Figure 1b, atomic force microscopy (AFM) measurement shows the nanosheets have area of several μm^2 and uniform thickness of 4–5 nm. Transmission electron microscope (TEM) measurement confirms the structure of the prepared Cu-TCPP nanosheets (Figure 1c).

Cu-TCPP nanosheets can be conveniently prepared to thin film in a layer-by-layer manner by our previously developed "modular assembly" method.[13a] For effectively modulating the proton current in H⁺-FET, a thin film with thickness less than 100 nm is preferred. Herein, the prepared ≈ 5.0 nm thick nanosheets enable us to control the thickness of the thin film more precisely than previous work.[13] 10 layer-by-layer deposition cycles resulted a ≈ 50 nm thin film (Figure S1). The in-plane patterns of grazing-incidence XRD (GIXRD) only show (*hk*0) peaks (Figure 2a), and the out-of-plane patterns show an (00*l*) peak (Figure 2b). This difference suggests the nanosheets in thin film lie parallel to the substrate with the *ab* plane.
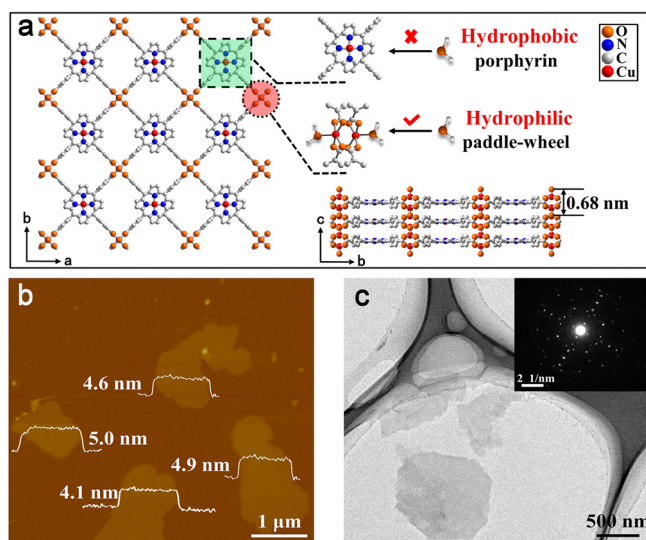
N₂ and Water vapor sorption measurements demonstrate that the existence of considerable number of interstitial nanospaces in Cu-TCPP thin film and also reveals their hydrophobicity (Figure S2).[11] These nanospaces run through with each other to form continuous two-dimensional nanochannels that parallel to the substrate. Time-dependent contact angle measurement (Figure 2c) reveal that the hydrophobic nanochannels can adsorb water due to the existence of large amount of hydrophilic sites. Moreover, SEM and XRD measurements demonstrate that the hydrophobic nature of the nanochannel can stabilize the thin film for 40 days in water (Figure 2d, S3 and S4). These features successfully mimic the features of bio-channel.

For H⁺-FET device fabrication, 50-nm Cu-TCPP thin film was deposited on a SiO₂/Si⁺ substrate with a pair of pre-
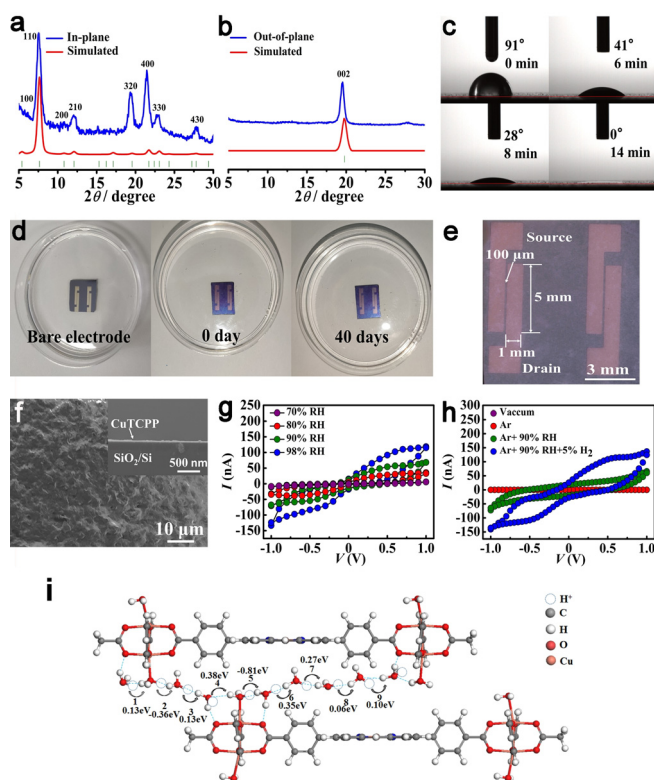
Figure 2. Characterizations of Cu-TCPP thin film (10 deposition cycles) H⁺-FETs. a) In-plane and b) out-of-plane XRD patterns. c) Contact angle measurement (the black rectangular object is a microinjector). d) Stability test. e) Optical image f) SEM image, inset: cross-sectional view. g) *I–V* curves under different RH and h) different atmospheres. i) DFT study of the proton-transport pathways and mechanism.

Figure 1. a) Crystal structure of Cu-TCPP. b) AFM and c) TEM image of Cu-TCPP nanosheets, inset: selected area electron diffraction pattern.

prepared 80-nm palladium (Pd) electrodes (Figure 2 e and f). Palladium was selected as the electrode material for its ability to continuously provide proton under H_2 atmosphere by forming PdH_x. PdH_x can conduct both electron and proton and thus affords effectively proton exchange with Cu-TCPP thin film under direct current (DC) condition.[3a] In this device, Cu-TCPP thin film is the active-layer, heavily doped Si substrate acts as the gate electrode, and two Pd (or PdH_x) electrodes are source and drain electrodes, respectively.

The proton transport in the Cu-TCPP active-layer was evaluated under different atmospheres via the DC method. As shown in Figure S3, the I–V curve recorded at vacuum has very small slope, revealing an electronic conductivity as low as 3.6×10^{-8} S cm^{-1} (details see ESI). Gradually increase the RH to 70% and then 98% in the air atmosphere, the conductivity increases to 4.1×10^{-5} and 5.4×10^{-4} S cm^{-1}, respectively (Figure 2 g). These values are similar to those determined by electrochemical impedance spectroscopy (EIS) under alternating current (AC) conditions in previous report.[11] Moreover, EIS study also reveals an activation energy of 0.28 eV for CuTCPP thin film, indicating a Grotthuss mechanism of proton transport.[11] Accordingly, a density functional theory calculation was performed to reveal more details on proton transport (details see supporting information). 8 water molecules sandwiched by two molecule fragments of CuTCPP were used as a typical model (Figure S5). It is found that the absorbed waters between the CuTCPP layers can be stabilized by forming hydrogen bonding network in the assistant of the hydrophilic points in the structure, which provides a continuous pathway for proton transfer. A proton injection to the hydrogen bonding network through electrode releases -1.49 eV (Figure S6), indicating that the injection process is favored in energy. Since the highest energy barrier for proton transport among adjacent water molecule is only 0.38 eV (Figure 2 i), protons can smoothly migrate under electrode field. Notably, the I–V curves circularly measured between -1 and 1 V are non-linear. They show bigger hysteresis and more declining loop at higher relative humidity (RH) condition. This phenomenon suggests higher conductivity and more ionic component appears in the charge carrier when increasing RH.[14] This is because more water molecules are adsorbed in the interstitial nanochannels under higher RH.[11] These water molecules would dissociate more mobile protons at the surface of Cu-TCPP nanosheets and construct more extensive hydrogen-bonding network to prompt proton transport. This hypothesis was demonstrated by adding 5% H_2 into Ar atmosphere with 90% RH to form PdH_x electrodes (Figure 2 h). Compared with the I–V curves measured without H_2, the I–V curve measured under 5% H_2 atmosphere shows similar change as the I–V curves measured with increased RH. The conductivity increased to 1.0×10^{-3} S cm^{-1} which is ≈ 2.7 times higher than the one without 5% H_2. It has been well known that the in situ formation of PdH_x can increase the concentration of the proton in channel of the device.[15] Meanwhile, I–V curves at 5% H_2 and 90% RH atmosphere show strong frequency-dependent behaviors (Figure S7). These are strong evidences for protonic current rather than electronic current because ionic motion has noticeable time relaxation while electron motion does not.[3a]

These results clearly evidence Cu-TCPP thin film is a feasible active-layer material to transport proton at DC condition.

Based on above results, the performance of Cu-TCPP thin film H$^+$-FET device was evaluated under the atmosphere of 90% RH and 5% H_2. Figure 3 a and b show the corresponding output and transfer curves, respectively. The protonic current in active-layer increases as the gate voltage negatively increases. Additionally, leakage current between source and gate electrodes was much lower than the current between source and drain electrodes, demonstrating the above effectively modulation was mainly attributed to the electric field effect of the device (Figure S8). The proton mobility in MOF protonic channel is estimated to be $\approx 9.5 \times 10^{-3}$ cm^2 V^{-1} s^{-1}. This value is higher than the mobilities of the typical H$^+$-FET made from maleic chitosan (4.9×10^{-3} cm^2 V^{-1} s^{-1}), reflectin (7.3×10^{-3} cm^2 V^{-1} s^{-1}) and porous organic polymer (5.7×10^{-3} cm^2 V^{-1} s^{-1}).[3a–c] The on-off ratio of Cu-TCPP thin film H$^+$-FET was ≈ 4.1 times, which is the maximum switching ratio in the reported H$^+$-FET within 10 V range (Figure S9). This high degree of modulation results from the variation of the proton concentration in MOF active-layer from 0.9×10^{17} cm^{-3} to 4.2×10^{17} cm^{-3} (Figure 3 c). Cu-TCPP thin film H$^+$-FETs also showed good stability and reproducibility (details see ESI, Figure S10, S11 and Table S1). Notably, although proton conducting MOFs have been extensively studied, this is the first time to report the proton mobility of MOFs and it is also the first report to physically and reversibly modulated the proton concentration in MOFs.[8]

The mechanism of the above physical modulation of proton concentration is attributed to electric field effect (Figure 3 d). When a negative gate voltage is applied to gate electrode, positive charges would be induced onto MOF active-layer due to dielectric capacitive coupling. Thus, additional protons are injected into the active-layer via PdH_x contacts to increase conductivity. Contrarily, when a positive gate voltage is applied, proton would be repelled from the active-layer and results lower conductivity. To demonstrate this mechanism, some comparison tests of the
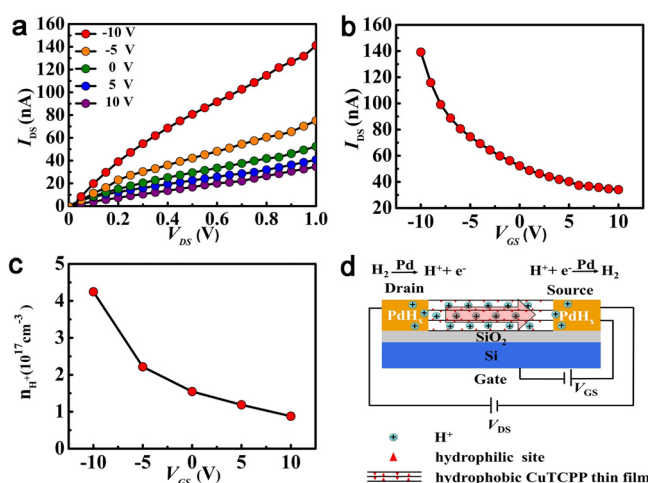
Figure 3. a) Configuration and working mechanism of Cu-TCPP H$^+$-FETs. b) Output and c) Transfer curves of Cu-TCPP H$^+$-FETs. d) Proton concentration in Cu-TCPP active-layer at different gate voltage.

H⁺-FET were performed without H_2. As results, no field-effect regulated current was observed in pure Ar or Ar with 90% RH atmosphere (Figure S12), because there is no additional proton could be provided from atmosphere to inject into the active-layer. This observation also further demonstrates that the modulated current is protonic current. Notably, whatever protons injected into or excluded from the MOF active-layer, one corresponding electron will be detected by external testing equipment when one proton crosses the contacted interface. Accordingly, the protonic current can be monitored directly.

In summary, MOF was demonstrated as a feasible high-performance active-layer material for bionic H⁺-FET for the first time. A 50-nm thick of MOF thin film with high crystallinity and orientation was constructed by reassembling ultra-thin Cu-TCPP nanosheets. The prepared MOF thin film possesses abundant two-dimensional interstitial nanochannels. With an elaborate structure design, these nanochannels possess hydrophobic nature while endowed with abundant hydrophilic sites. This unique structure enables the film to adsorb water in nanochannel while keep its stability in water, which facilitates to more proximally mimic the proton transport in biological channel than the reported H⁺-FETs. As results, the prepared devices show proton mobility of 9.5×10^{-3} $cm^2 V^{-1} s^{-1}$ and on-off ratio of 4.1, both of which are the highest values in the reported works. This work not only provides an effective way to physically and reversibly regulating the proton transport of MOF materials for the first time, but also takes an important step forward for extending the application of MOF materials to bionic electronics.

Conflict of interest

The authors declare no conflict of interest.

[1] a) M. L. Björck, P. Brzezinski, *Nat. Commun.* **2018**, *9*, 3187; b) M. Kataoka, H. Kamikubo, *Biophys. Physicobiol.* **2019**, *16*, 274–279; c) R. Davydov, S. Chemerisov, D. E. Werst, T. Rajh, T. Matsui, M. Ikeda-Saito, B. M. Hoffman, *J. Am. Chem. Soc.* **2004**, *126*, 15960–15961.

[2] W. Guo, Y. Tian, L. Jiang, *Acc. Chem. Res.* **2013**, *46*, 2834–2846.

[3] a) C. Zhong, Y. X. Deng, A. F. Roudsari, A. Kapetanovic, M. P. Anantram, M. Rolandi, *Nat. Commun.* **2011**, *2*, 476; b) D. D. Ordinario, L. Phan, W. G. Walkup IV, J.-M. Jocson, E. Karshalev, N. Hüsken, A. A. Gorodetsky, *Nat. Chem.* **2014**, *6*, 596–602; c) H. Zhong, G. D. Wu, Z. H. Fu, H. W. Lv, G. Xu, R. H. Wang, *Adv. Mater.* **2020**, *32*, 2000730; d) Z. Hemmatian, T. Miyake, Y. Deng, E. Josberger, S. Keene, R. Kautz, C. Zhong, J. Jin, *J. Mater. Chem. C* **2015**, *3*, 6407–6412; e) T. Miyake, M. Rolandi, *J. Phys. Condens. Matter* **2016**, *28*, 023001.

[4] X. Strakosas, J. Selberg, Z. Hemmatian, M. Rolandi, *Adv. Sci.* **2017**, *4*, 1600527.

[5] a) K. Murata, K. Mitsuoka, T. Hirai, T. Walz, P. Agre, J. B. Heymann, A. Engel, Y. Fujiyoshi, *Nature* **2000**, *407*, 599–605; b) H. X. Sui, B. G. Han, J. K. Lee, P. Walian, B. K. Jap, *Nature* **2001**, *414*, 872–878.

[6] a) H. Furukawa, K. E. Cordova, M. O'Keeffe, O. M. Yaghi, *Science* **2013**, *341*, 1230444; b) H. C. Zhou, J. R. Long, O. M. Yaghi, *Chem. Rev.* **2012**, *112*, 673–674; c) H. C. Zhou, S. Kitagawa, *Chem. Soc. Rev.* **2014**, *43*, 5415–5418.

[7] a) X. Zhao, Y. X. Wang, D. S. Li, X. H. Bu, P. Y. Feng, *Adv. Mater.* **2018**, *30*, 1705189; b) M. Zhao, S. Ou, C. D. Wu, *Acc. Chem. Res.* **2014**, *47*, 1199–1207; c) K. J. Lee, J. H. Lee, S. Jeoung, H. R. Moone, *Acc. Chem. Res.* **2017**, *50*, 2684–2692; d) T. Kundu, M. Wahiduzzaman, B. B. Shah, G. Maurin, D. Zhao, *Angew. Chem. Int. Ed.* **2019**, *58*, 8073–8077; *Angew. Chem.* **2019**, *131*, 8157–8161; e) X. C. Cai, Z. X. Xie, D. D. Li, M. Kassymova, S. Q. Zang, H. L. Jiang, *Coord. Chem. Rev.* **2020**, *417*, 213366; f) W. H. Li, W. H. Deng, G. E. Wang, G. Xu, *EnergyChem* **2020**, *2*, 100029; g) W. P. Lustig, S. Mukherjee, N. D. Rudd, A. V. Desai, J. Li, S. K. Ghosh, *Chem. Soc. Rev.* **2017**, *46*, 3242–3285; h) I. Stassen, N. C. Burtch, A. A. Talin, P. Falcaro, M. D. Allendorf, *Chem. Soc. Rev.* **2017**, *46*, 3185–3241.

[8] a) D.-W. Lim, H. Kitagawa, *Chem. Rev.* **2020**, *120*, 8416–8467; b) M. Sadakiyo, T. Yamada, H. Kitagawa, *J. Am. Chem. Soc.* **2009**, *131*, 9906–9907; c) J. M. Taylor, R. K. Mah, I. L. Moudrakovski, C. I. Ratcliffe, *J. Am. Chem. Soc.* **2010**, *132*, 14055–14057; d) S. C. Sahoo, T. Kundu, R. Banerjee, *J. Am. Chem. Soc.* **2011**, *133*, 17950–17958; e) Y. X. Ye, W. G. Guo, L. H. Wan, Z. Y. Li, Z. J. Song, J. Chen, Z. J. Zhang, S. C. Xiang, B. L. Chen, *J. Am. Chem. Soc.* **2017**, *139*, 15604–15607; f) D. X. Gui, X. Dai, Z. T. Tao, T. Zheng, X. X. Wang, M. A. Silver, J. Shu, L. H. Chen, Y. L. Wang, T. T. Zhang, J. Xie, L. Zou, Y. H. Xia, J. J. Zhang, J. Zhang, L. Zhao, J. Diwu, R. H. Zhou, Z. F. Chai, *J. Am. Chem. Soc.* **2018**, *140*, 6146–6155; g) F. M. Zhang, L. Z. Dong, J. S. Qin, W. Guan, J. Liu, S. L. Li, M. Lu, Y. Q. Lan, Z. M. Su, H. C. Zhou, *J. Am. Chem. Soc.* **2017**, *139*, 6183–6189; h) S. Horike, D. Umeyama, S. Kitagawa, *Acc. Chem. Res.* **2013**, *46*, 2376–2384.

[9] a) S. Kim, B. Joarder, J. A. Hurd, J. F. Zhang, K. W. Dawson, B. S. Gelfand, N. E. Wong, G. K. H. Shimizu, *J. Am. Chem. Soc.* **2018**, *140*, 1077–1082; b) S. S. Liu, Z. Han, J. S. Yang, S. Z. Huang, X. Y. Dong, S. Q. Zang, *Inorg. Chem.* **2020**, *59*, 396–402; c) Q. Tang, Y. W. Liu, S. X. Liu, D. F. He, J. Miao, X. Q. Wang, G. C. Yang, Z. Shi, Z. P. Zheng, *J. Am. Chem. Soc.* **2014**, *136*, 12444–12449; d) Y. S. Wei, X. P. Hu, Z. Han, X. Y. Dong, S. Q. Zang, T. C. W. Mak, *J. Am. Chem. Soc.* **2017**, *139*, 3505–3512.

[10] a) M. T. Zhao, Y. X. Wang, Q. L. Ma, Y. Huang, X. Zhang, J. F. Ping, Z. C. Zhang, Q. P. Lu, Y. F. Yu, H. Xu, Y. L. Zhao, H. Zhang, *Adv. Mater.* **2015**, *27*, 7372–7378; b) Y. W. Zhao, J. Wang, R. J. Pei, *J. Am. Chem. Soc.* **2020**, *142*, 10331–10336; c) Y. Lu, S. Q. Zhang, S. L. Dai, D. P. Liu, X. Wang, W. Tang, X. J. Guo, J. Duan, W. Luo, B. B. Yang, J. Zou, Y. H. Huang, H. E. Katz, J. Huang, *Matter* **2020**, *3*, 904–919.

[11] G. Xu, K. Otsubo, T. Yamada, S. Sakaida, H. Kitagawa, *J. Am. Chem. Soc.* **2013**, *135*, 7438–7441.

[12] S. Motoyama, R. Makiura, O. Sakata, H. Kitagawa, *J. Am. Chem. Soc.* **2011**, *133*, 5640–5643.

[13] a) G. Xu, T. Yamada, K. Otsubo, S. Sakaida, H. Kitagawa, *J. Am. Chem. Soc.* **2012**, *134*, 16524–16527; b) J. X. Liu, C. Woll, *Chem. Soc. Rev.* **2017**, *46*, 5730–5770.

[14] a) S. De, C. Cramer, M. Schonhoff, *Macromolecules* **2011**, *44*, 8936–8943; b) D. W. Lim, M. Sadakiyo, H. Kitagawa, *Chem. Sci.* **2019**, *10*, 16–33.

[15] H. Morgan, R. Pethig, G. T. J. Stevens, *Phys. E Sci. Instrum.* **1986**, *19*, 80–82.